

# 1 **Determining groundwater degradation from irrigation in desert-marginal** 2 **northern China**

3 Brighid E. Ó Dochartaigh<sup>1a</sup>, Alan M. MacDonald<sup>1</sup>, William G. Darling<sup>2</sup>, Andrew G. Hughes<sup>3</sup>, Jin X.  
4 Li<sup>4</sup> and Li A. Shi<sup>5</sup>

5 <sup>1</sup> British Geological Survey, Murchison House, West Mains Road, Edinburgh EH9 3LA, United Kingdom

6 <sup>2</sup> British Geological Survey, Maclean Building, Crowmarsh Gifford, Wallingford, Oxon OX10 8BB, United  
7 Kingdom

8 <sup>3</sup> British Geological Survey, Kingsley Dunham Centre, Keyworth, Nottingham NG12 5GG, United Kingdom

9 <sup>4</sup> Division of Hydrology and Water-Land Resources, Cold and Arid Regions Environmental and Engineering  
10 Research Institute, CAS, 260 Donggang West Rd., Lanzhou, 730000, Gansu, China

11 <sup>5</sup> Alxa League AusAID Project Management Office, Bayanhot, 750306, Inner Mongolia, China

12 <sup>a</sup> Corresponding author: [beod@bgs.ac.uk](mailto:beod@bgs.ac.uk) ; Telephone +44 (0)131 650 0424; Fax +44 (0)131 650 0252

13

## 14 **Abstract**

15 Groundwater degradation from irrigated agriculture is of concern in semi-arid northern China. Data-scarcity  
16 often means the causes and extent of problems aren't fully understood. This study investigated an irrigated area  
17 in Inner Mongolia where abstraction from an unconfined Quaternary aquifer has increased threefold over 20  
18 years to 20 Mcm/yr; groundwater levels are falling at up to 0.5 m/yr; and groundwater is increasingly  
19 mineralised (TDS increase from 400 mg/L to 700–1900 mg/L), with nitrate concentrations up to 137 mg/L-N.  
20 Residence-time (chlorofluorocarbon/CFC), stable-isotope and hydrogeochemical indicators helped develop a  
21 conceptual model of groundwater system evolution, demonstrating a direct relationship between modern water  
22 proportion and the degree of groundwater mineralisation, indicating that irrigation water recycling is reducing  
23 groundwater quality. The investigations suggest that before irrigation development, active recharge to the  
24 aquifer from wadis significantly exceeded groundwater inflow from nearby mountains, previously held to be the  
25 main groundwater input. Away from active wadis, groundwater is older with a probable pre-Holocene  
26 component. Proof-of-concept groundwater modelling supports geochemical evidence, indicating the importance  
27 of wadi recharge and irrigation return flows. Engineering works protecting the irrigated area from flooding have  
28 reduced good quality recharge; active recharge is now dominated by irrigation returns, which are degrading the  
29 aquifer.

30 **Introduction**

31 Groundwater is the primary source of water in most of arid northern China, with the largest use being  
32 for irrigation (Kendy et al. 2003). Low rainfall and high evapotranspiration mean surface water  
33 resources are scarce. Groundwater is subject to increasing abstraction pressure as a result of rapid  
34 population and economic growth (e.g. Foster et al. 2004, Ji et al. 2006).

35

36 The detrimental impacts of irrigated agriculture on groundwater resources in northern China are  
37 widely recognised (Foster et al 2004, Ma et al 2005, Ji et al 2006). Intensive abstraction has caused  
38 widespread water table decline, such as in parts of the North China Basin, where Kendy et al. (2003)  
39 report that groundwater levels are falling by more than 1.0 m/yr. Severe groundwater quality  
40 degradation has also occurred beneath many irrigated areas, linked to the recycling of salts from  
41 irrigation water, and particularly to nitrate from intensive fertiliser use (e.g. Chen et al. 2005, Ji et al.  
42 2006). As water tables fall, groundwater abstraction becomes more difficult and expensive, and  
43 eventually wells may dry up. As its quality deteriorates, groundwater may become unsuitable for  
44 higher quality uses.

45

46 This paper investigates the causes and impacts of groundwater degradation in a Quaternary aquifer in  
47 an irrigated area, Chahaertan, in Inner Mongolia in northern China. Few groundwater data are  
48 available for this region, and to address this, a range of hydrogeological techniques was applied to  
49 investigate and interpret the local groundwater system and how it has developed historically in  
50 response to the expansion of abstraction for irrigation. This approach, particularly related to  
51 groundwater residence times and the historical development of groundwater systems, complements  
52 the recently growing body of hydrogeological work in China by advancing the focus on managing  
53 groundwater resources and irrigated agriculture.

54

55 The Chahaertan irrigated area lies between longitude 105° 37' to 105° 45' E and latitude 39° 14' to  
56 39° 29' N, at an elevation of between 1100 and 1200 m above sea level (asl) (Figure 1). This region,

57 near the eastern edge of the Tengere desert, is semi-arid and characterised by low, irregular rainfall  
58 and high temperatures and evapotranspiration (Ma et al. 2005). Land use is dominated by scrub  
59 grassland, much of it degraded, and sandy desert, with some limited forest cover. Areas under  
60 irrigation, such as Chahaertan, account for a small proportion of the total land area, but are significant  
61 in terms of human and economic activity. At Chahaertan, more than 150 wells support intensive  
62 seasonal groundwater abstraction to irrigate commercial crops: dominantly maize, sunflowers and  
63 watermelon, with increasing amounts of cotton. Almost all groundwater abstraction is for irrigation  
64 and occurs between April and August. Away from the irrigated area there are only a handful of wells  
65 across the rest of the Quaternary aquifer, which abstract at low rates for domestic and small-scale  
66 livestock use.

67

68 By the mid 2000s it was suspected that intensive abstraction at Chahaertan was having a detrimental  
69 effect on the groundwater resource. However, because no monitoring or investigations had been  
70 carried out since the mid 1990s (Yuan and Wu 1996), a lack of hydrogeological data and  
71 understanding precluded the establishment of an effective management strategy. The common theory  
72 at this time held that the major groundwater input to the local Chahaertan system was slow lateral  
73 flow through the aquifer from its southern boundary, where focussed recharge occurred from surface  
74 water flowing from the Helan Mountains (Figures 1 and 2) (Yuan and Wu 1996). However, this did  
75 not explain many of the observed system features.

76

### 77 **New groundwater investigations**

78

79 In 2006 an investigation was carried out at Chahaertan to collate existing and collect new essential  
80 information and improve understanding of the groundwater system and the state of the groundwater  
81 resource, and to provide the basis for effective resource management. To deal with the lack of  
82 historical hydrogeological and hydrological data, a set of complementary hydrogeological and

83 hydrogeochemical techniques, including detailed groundwater residence time analysis using CFCs,  
84 was used to establish a comprehensive picture of the groundwater system.

85

86 More than 150 abstraction wells in Chahaertan were accurately located using GPS, and a  
87 questionnaire used to collect information from well owners to help document historical groundwater  
88 development and estimate current groundwater abstraction.

89

90 Historical groundwater level measurements were located for six monitoring wells in the main irrigated  
91 area for the period 1984–94, and new measurements made in these wells in September 2006. All are  
92 close to abstraction wells and affected by pumping. Additional water level measurements were made  
93 in abstraction wells across the irrigated area. Outside this area there are limited historical data for the  
94 Quaternary aquifer, but what were available were collated from hydrogeological maps and reports,  
95 and where possible new measurements were also made in available (usually pumping) wells.

96

97 Meteorological data were obtained from government meteorological records and research stations,  
98 published reports, and previous studies (e.g. Yuan and Wu 1996, People’s Liberation Army 1976 and  
99 1980). Additional information on aquifer geology, geometry and hydraulic properties, and well yields  
100 was collated from records, reports and maps from a variety of sources (e.g. People’s Liberation Army  
101 1976, 1980; Left Banner Water Management and Water Resource Office 1992; Yuan and Wu 1996).

102

103 Twenty two groundwater samples were collected from the Quaternary aquifer: 19 from the irrigated  
104 area (including two from a separate zone to the north of the main irrigated area, called Little  
105 Chahaertan), and three from the surrounding un-irrigated aquifer (Figure 3). All except one of the  
106 samples were collected from pumped abstraction wells, the remaining one being collected from a  
107 flowing artesian well. Technical details of sample collection are given in Ó Dochartaigh and  
108 MacDonald (2006). Proof of concept numerical modelling was used to test the results of the  
109 hydrodynamic and hydrogeochemical (including residence time) analysis and the conceptual  
110 understanding of the groundwater system.

111

112 **The hydrogeology of Chahaertan and the development of irrigation and the**  
113 **groundwater system**

114

115 Irrigation wells at Chahaertan abstract from an unconfined Quaternary alluvial aquifer infilling a  
116 faulted basin in Cretaceous and Tertiary rocks. The southern edge of the aquifer basin is faulted  
117 against the Helan Mountains, ~30 km southeast of Chahaertan; the northern boundary of the  
118 groundwater catchment is at Jilantai lake, ~35 km north of Chahaertan, which is the main discharge  
119 point for surface water and groundwater in the catchment (Figure 1). The total groundwater catchment  
120 area is ~1500 km<sup>2</sup>. Aquifer thickness varies from less than 30 m at its southern edge to more than 200  
121 m around Chahaertan (Figure 2), and possibly deeper at Jilantai. Surface elevation ranges from over  
122 3000 m asl at the top of the Helan Mountains to 1000 m asl at Jilantai. Near to Jilantai the aquifer  
123 becomes confined in some areas. The exact extent of artesian conditions is unknown, but the  
124 approximate extent has been estimated (Figure 1) by the presence of vegetation and salt encrustation  
125 in unirrigated areas visible on satellite imagery.

126

127 Basin infill is dominated by fluvial sediment eroded from the Helan Mountains and transported  
128 northwestwards by high-energy ephemeral rivers (wadis) (Figure 2). Previous studies showed that  
129 aquifer hydraulic properties are strongly influenced by sediment grain size variation, with generally  
130 coarser-grained deposits proximal to the Helan Mountains showing a transmissivity range of 600 to  
131 1200 m<sup>2</sup>/d, and finer-grained distal deposits around Chahaertan a range of 200 to 510 m<sup>2</sup>/d  
132 (Groundwater Development and Utilisation Teaching and Research Office 1984, Yuan and Wu,  
133 1996). There are no available data on aquifer mineralogy.

134

135 Outside the irrigated area there is little soil development, and the region is dominated by sand with  
136 thin scrub vegetation. Prior to irrigation development, however, seasonal overbank flooding at  
137 Chahaertan at the confluence of wadis draining the Helan Mountains led to significant soil

138 development (Groundwater Development and Utilisation Teaching and Research Office 1984, Jerie  
139 2006).

140

141 Long-term average (LTA) rainfall at Chahaertan is some 200 mm/yr; over the Helan Mountains to the  
142 south it is 400 mm/yr, falling to 100 mm/yr at Jilantai to the north. Most precipitation falls between  
143 June and September as short-lived intensive events. Mean annual potential evaporation ranges from  
144 1400 mm in the mountains to 3000 mm at Jilantai, and is highest between May and August. The  
145 temperature at Chahaertan exceeds 30°C in summer but is typically below 0°C in winter, with an  
146 annual mean of ~15°C (e.g. Yuan and Wu 1996, People's Liberation Army 1976 and 1980).

147

148 There is no permanent surface water drainage. Wadis drain runoff from the Helan Mountains  
149 northwest towards Jilantai, four of which converge to the south of Chahaertan, from where a single  
150 channel flows north to Jilantai. No river flow monitoring is carried out in the region, but there is  
151 anecdotal evidence for channel flows at Chahaertan and Jilantai. Based on this and on the size of the  
152 river channel, gradient and depth (Table I), the river flow rate during these events is estimated at  
153 between 20 and 30 m<sup>3</sup>/sec.

154

155 Overall groundwater flow direction in the Quaternary is from the south and southeast to the north.  
156 Natural groundwater discharge is to the lake at Jilantai and to springs and seepages in this area, seen  
157 in the distribution of artesian conditions (Figure 1). At Chahaertan, groundwater flows are likely to be  
158 influenced by local indirect recharge and by intensive groundwater abstraction.

159

160 Since initial development in the late 1960s, the number of abstraction wells, volume of groundwater  
161 abstraction, and irrigated area at Chahaertan have increased markedly (Figure 4) (data from  
162 Groundwater Development and Utilisation Teaching and Research Office 1984, Left Banner Water  
163 Management and Water Resource Office 1992). Since 1990, most new wells have been drilled in  
164 Little Chahaertan, just north of the main irrigated area (Figure 4).

165

166 In 2006 groundwater levels ranged from 45 m below ground level (mbgl) at the northern edge of the  
167 main irrigated area to more than 75 mbgl some 8.5 km away in the south, this slope being largely  
168 controlled by topography. The only available historical monitoring data show that groundwater levels  
169 in this area fell by an average of 0.5 m/yr between 1984 and 1995, a decline that apparently continued  
170 until 2006, albeit at a slightly slower rate (Figure 4). This is likely to be linked to the slow-down in  
171 the rate of increase of abstraction in this area after the shift in focus for groundwater development to  
172 Little Chahaertan (where there has been no groundwater level monitoring) after 1990.

173

174 Regular groundwater quality monitoring has never been undertaken at Chahaertan, but the limited  
175 available data indicate that pre-development groundwater chemistry is likely to have been similar to  
176 groundwater today in the surrounding non-irrigated area: moderately mineralised, Ca-Mg dominated  
177 waters with slightly alkaline pH, and less than 5 mg/L NO<sub>3</sub>-N. By 2006, TDS concentrations in the  
178 irrigated area were between 700 and 1900 mg/L, and nitrate concentrations reached up to 137 mg/L as  
179 N. Nitrogen isotope analysis has shown that the bulk of this nitrate derives from fertiliser (Jerie 2006).

180

181 Irrigation development at Chahaertan was heavily dependent on its position at the confluence of four  
182 wadis and consequent local seasonal overbank flooding and soil development (Groundwater  
183 Development and Utilisation Teaching and Research Office 1984). Since development, however, the  
184 wadi channels have been engineered, including major re-routing of the original confluent channel  
185 from the centre to the western edge of the irrigated area, which has largely prevented flooding, and  
186 consequent crop and livelihood damage, in the now intensively farmed area.

187

## 188 **Groundwater chemistry**

189

190 An understanding of groundwater chemistry has been critical in revealing changing recharge  
191 processes at Chahaertan. Groundwater chemistry has been interpreted from the 22 samples collected  
192 from abstraction wells in the irrigated area and surrounding region. The average length of the

193 screened section of the production wells from which samples were collected is 45 m (Left Banner  
194 Water Management and Water Resource Office 1992). The locations and field measurements of  
195 chemistry samples are given in Table ESM1, and locations are shown in Figure 3. Major and minor  
196 inorganic species are reported in Table ESM2. Stable isotope and CFC analyses are provided in Table  
197 ESM3.

198

#### 199 *Pre-development groundwater chemistry*

200 The nature of an intensively irrigated area means that little groundwater is likely to be fully  
201 representative of pre-development water quality, and therefore of natural processes operating along  
202 the groundwater flowline. No pre-development chemistry data for the aquifer are available, but seven  
203 of the new groundwater samples are likely to represent quasi-natural conditions. Three of these (Sites  
204 20, 21 and 22) are away from any irrigation and outside the local Chahaertan groundwater system;  
205 four (Sites 4 and 16 in Chahaertan, and 18 and 19 in Little Chahaertan) are within the irrigated area  
206 (Figure 3). Site 22, away from any irrigation and unlikely to be influenced by agricultural or other  
207 contamination, has a NO<sub>3</sub>-N concentration of 5.6 mg/L and a TDS of ~450 mg/L. This is likely to be  
208 indicative of pre-development chemistry: arid area groundwaters frequently have detectable NO<sub>3</sub>-N  
209 originating from sources such as atmospheric deposition, bacteria in soil crusts, and termite mounds  
210 (Gates et al. 2008). All four probable quasi-natural groundwater samples within the irrigated area  
211 show similar NO<sub>3</sub>-N concentrations of <5 mg/L.

212 These pre-development groundwaters are Ca-Mg dominated and moderately mineralised, with an  
213 average TDS of 395 mg/L, well oxygenated, with a slightly alkaline pH, and noticeably lower  
214 concentrations of all major ions (except HCO<sub>3</sub>), than the other Chahaertan waters (Tables ESM1,  
215 ESM2). They are comparable to a similar Quaternary alluvial aquifer in the semi-arid Datong Basin in  
216 northwest China, where groundwaters unaffected by agriculture or industry had an average TDS of <  
217 300 mg/l and NO<sub>3</sub>-N concentration of 7.3 mg/l (Guo and Wang 2004).

218



219 The sampled wells consistently show evolution in key species in the downstream flow direction from  
220 Chahaertan to Jilantai (Figure 5). The increase in Na as Ca decreases is typical of ion exchange, but  
221 the greater magnitude of Na enrichment compared to the Ca decline (Figure 6a) suggests an additional  
222 source of Na. Evidence from Br/Cl ratios (Figure 6b) indicates this could be halite dissolution, but in  
223 the absence of any mineralogical data for the aquifer this cannot be confirmed. From Site 19  
224 northwards, Cl and SO<sub>4</sub> concentrations increase at the expense of HCO<sub>3</sub>. The increase in Cl is  
225 consistent with halite dissolution. The SI<sub>gypsum</sub> values are two orders of magnitude below saturation  
226 (Table ESM2), indicating gypsum dissolution as the cause of the increase in SO<sub>4</sub>. The excess Ca  
227 initially produced may have been taken up by ion exchange and/or precipitation of calcite due to  
228 solubility considerations.

229

### 230 *Irrigation-related changes to groundwater chemistry*

231 Sites 1–17 are all within the main irrigated area and all show evidence of irrigation-related changes in  
232 groundwater chemistry (excluding Sites 4 and 16 discussed above). The groundwaters are well-  
233 oxygenated, with pH values in the range 7.4–8.0, and are significantly more mineralised than the pre-  
234 development group, with an average TDS of 1156 mg/L, and generally at least double the  
235 concentrations of major ions (Table ESM2). The average NO<sub>3</sub>-N concentration is 27.9 mg/L, more  
236 than seven times that of the average in the pre-development group. This compares with evidence from  
237 similar irrigated aquifers in northwest China, where TDS is >800 mg/L and NO<sub>3</sub>-N >23 mg/L (Guo  
238 and Wang 2004).

239

240 Multi-plots versus Cl of the main ions (Figure 7) show generally good correlations, positive for Ca,  
241 Na and SO<sub>4</sub>, and negative for HCO<sub>3</sub>, with Site 4 (quasi-natural water) having the least-modified  
242 composition. The linear increases can be attributed to the effects of groundwater mixing with  
243 evaporated irrigation return water. The decrease in HCO<sub>3</sub> is consistent with the loss of CO<sub>2</sub> during  
244 recycling, and therefore a tendency towards calcite precipitation, supported by the positive correlation  
245 ( $r^2 = 0.44$ ) between SI<sub>calcite</sub> and pH (Table ESM2). Nitrate has the poorest correlation with Cl, which  
246 is probably a consequence of biotic effects.

247

## 248 **Groundwater residence time**

249

### 250 *Pre-development groundwater residence times*

251 CFC analyses are only available for two pre-development samples: Sites 4 and 19 (Table ESM3).

252 CFC-11 and CFC-12 are both below detection at Site 19 in Little Chahaertan, indicating no evidence

253 of modern water. This is likely to reflect the smaller influence of focussed recharge from pre-

254 development overbank flooding north of the main Chahaertan area (Figure 1). Site 4 shows evidence

255 of modern water, indicating active modern recharge, which is likely to derive largely from pre-

256 development flooding and leakage through wadi beds. Recharge modelling to confirm this hypothesis

257 is discussed in a subsequent section.

258

259 Stable isotopes in groundwaters from Chahaertan are too depleted to represent local groundwater

260 recharge from modern rainfall at this altitude. The presence of CFCs and the fact that stable isotopes

261 at Site 4 are less depleted than in the likely pre-Holocene waters further north along the flow line

262 (Sites 18 and 20; Figure 8), imply that pre-development groundwater at Chahaertan is not particularly

263 old, and unlikely to be pre-Holocene. The isotopic composition of end-Pleistocene groundwater is

264 based on a 2‰ depletion in  $\delta^{18}\text{O}$ , as found by Kreuzer et al. (2009) in the North China Plain (Figure

265 8). The most likely source of recharge is rainfall runoff from the Helan Mountains, where the higher

266 altitude creates cooler recharge conditions. The likely presence of pre-development modern water at

267 Chahaertan implies the recharge route is local river infiltration, as the travel time for groundwater

268 flow to Chahaertan from recharge at the edge of the mountains is estimated at ~5kyr, based on

269 reported or estimated aquifer hydraulic properties and Darcy's law (assuming a hydraulic gradient of

270 0.003 (Yuan and Wu 1996) and a hydraulic conductivity of 5 m/d).

271

272 When interpreting the patterns in CFC-12 and  $\delta^{18}\text{O}$  in downgradient samples (Figure 9) in terms of an

273 evolutionary sequence, key evidence is the below detection CFC-12 at Site 20, some 30 km north of

274 Chahaertan, and the presence of well oxygenated water, which argues against any microbial  
275 degradation (e.g. Busenberg and Plummer 1992). It is therefore assumed that groundwater at Site 20  
276 is more than 50 years old, which suggests that the main recharge area is at Chahaertan, with no  
277 modern recharge downgradient of Chahaertan. This is supported by  $\delta^{18}\text{O}$  values, which show a steady  
278 decline between Sites 4 and 20, of the order of 2 ‰, indicating that the flowline is long enough to  
279 retain some Pleistocene (>10 kyr) water in the system. By comparison, in the North China Plain  
280 similar depletions in  $\delta^{18}\text{O}$  were observed for late Pleistocene palaeowaters (Chen et al. 2003).

281

282 However, the data for Site 21 at Jilantai indicate a proportion of modern water is present (Figure 9).  
283 This borehole is drilled beneath Jilantai lake, and groundwater abstracted from the borehole is  
284 discharged into the lake, which is likely to locally reverse the hydraulic gradient and cause some re-  
285 infiltration of lake water into the aquifer.

286

#### 287 *Irrigation-related changes to groundwater residence*

288 CFC data indicate that most of the sampled groundwaters have a modern water component of 5–10%.  
289 A plot of CFC-11 versus CFC-12 concentrations is superimposed with the expected ‘piston flow’  
290 concentration curve relating to the year of recharge and the expected mixing line between modern and  
291 older CFC-free water (Figure 10). In practice, where the two lines are close together it is impossible to  
292 discriminate between piston flow and mixing. Additionally, there is evidence for a small amount of  
293 CFC-12 contamination in some samples, most notably Sites 1 and 4. The alternative explanation of  
294 CFC-11 reduction is unlikely based on the observed positive dissolved oxygen concentrations.  
295 Modern recharge could be from two sources: wadi flow or irrigation return water (which would  
296 acquire a modern CFC load while exposed to the atmosphere). The positive correlation between CFC-  
297 11 (presumed to be uncontaminated) and TDS (total dissolved solids) (Figure 11) suggests that  
298 irrigation return water is the more likely source. Site 4 lies outwith this trend, indicating that it is not  
299 impacted by irrigation returns, and further supporting its quasi-natural status.

300

301 Stable isotopes from Chahaertan groundwaters are tightly grouped (the standard deviation on  $\delta^{18}\text{O}$  is  
302 0.22 ‰), but the average is slightly beneath the Yinchuan meteoric line (Figure 8). This suggests there  
303 has been minor evaporative fractionation, consistent with the evidence of recycling demonstrated by  
304 the groundwater chemistry and CFCs. The average composition, at around  $-11$  ‰  $\delta^{18}\text{O}$  and  $-80$  ‰  
305  $\delta^2\text{H}$ , is significantly depleted compared to the Yinchuan average (Figure 8). Since Yinchuan is at an  
306 elevation of 1100 m asl, similar to Chahaertan, this implies the source of recharge at Chahaertan lies  
307 at a significantly higher altitude. The hydrodynamic factors of the system mean this source can only  
308 be the Helan Mountains, as for the pre-development water. This has subsequently been recycled as  
309 irrigation water.

310

### 311 **Testing results using groundwater modelling**

312

313 Proof of concept numerical modelling was used to test the results of the hydrodynamic and  
314 hydrogeochemical (including residence time) analysis and the conceptual understanding of the  
315 groundwater system. The scarcity of hydrogeological data and, therefore, limited conceptual  
316 understanding, means that numerical modelling can only support the development of the  
317 understanding of the groundwater system. It cannot provide a detailed simulation of the system (for  
318 example, for use as a management tool for assessing the impact of individual production wells)  
319 without significantly more information than is currently available.

320

#### 321 *Model set up*

322 Modelling was undertaken using the ZOOM (Zoomable Object Oriented Model) suite of object-  
323 oriented numerical groundwater models (Spink et al. 2003; Spink et al. 2006). This includes a  
324 distributed recharge model, ZOODRM (Zoomable Object Oriented Distributed Recharge Model) (e.g.  
325 Hughes et al. 2006, Hughes et al. 2008), which calculates spatial and temporal variations in  
326 groundwater recharge, incorporating a standard Penman-Grindley type soil moisture balance method,  
327 the modified FAO Penman-Monteith method (Allen et al. 1998), and procedures for recharge

328 estimation in arid countries (a “Wetting Threshold” method based on the work of Lange et al., 2003;  
329 Hughes et al., 2008) and irrigated regions, as well as surface runoff routing. The ZOOM suite also  
330 includes a groundwater flow model, ZOOMQ3D (Zoomable Object Oriented Model for Quasi-Three  
331 Dimensional Flow) (e.g. Jackson et al. 2005), which incorporates mesh refinement to aid the solution  
332 of scale-related problems, and is based on object-oriented techniques.

333

334 A detailed description of model development and input parameters is given in Ó Dochartaigh and  
335 MacDonald (2006). A distributed recharge model was developed encompassing the Quaternary  
336 aquifer catchment and the surface water catchment on the northern side of the Helan Mountains that  
337 drains towards Jilantai, taking into account the discharge zone in the area around Jilantai (Figure 12).  
338 The model area is 43 km by 83 km (Figure 12) with a cell size of 1000 m. Using data on daily  
339 rainfall, potential evaporation, land-use and topography, the model simulates LTA recharge based on  
340 average climatic data for the periods 1955-1980 and 2003-2005. It uses a wetting threshold method  
341 that is appropriate to arid and semi-arid conditions (Lange et al. 2003, Hughes et al. 2008). Two zones  
342 for wetting threshold were chosen: the outcrop of Quaternary and Tertiary age rocks. Indirect  
343 recharge was provided by including run-off processes to the wadis deriving the aspect direction from  
344 the DEM. Further information on the recharge model boundary conditions, model parameters, input  
345 and output and validation data is presented in Table ESM4.

346

347 A steady state groundwater flow model was developed to encompass the Quaternary basin aquifer  
348 within the Jilantai catchment area (Figure 12), simulating the groundwater system for a single year  
349 under 2006 conditions (Figure 13), and using calculated LTA recharge from the distributed recharge  
350 model. The groundwater flow model is a single layer model with an identical size and mesh to the  
351 recharge model. Inflows are rainfall recharge, indirect recharge from wadis and irrigation returns,  
352 which are provided directly from the recharge model. Outflows are from abstractions and  
353 groundwater discharge to the Jilantai Lake. Transmissivity and storage coefficients are distributed  
354 based on information from the available literature (e.g. Groundwater Development and Utilisation  
355 Teaching and Research Office, 1984). Further information on the groundwater flow model boundary

356 conditions, model parameters, input and validation data is presented in Table ESM5. Subsequently, a  
357 dynamic balance groundwater flow model was developed to investigate the time variant nature of the  
358 system, representing a 30 year period from 1980 to 2010, and using monthly varying recharge from  
359 the recharge model (Table ESM5). A dynamic balance is achieved by inputting a repeated annual  
360 series of average monthly recharge. The repeated annual series is run through the model until the  
361 groundwater heads in each month are identical to those in the same month in the previous year  
362 (Rushton and Wedderburn 1971).

363

#### 364 *Model results*

365 The recharge model was refined so the simulated river flows fit closely the available estimates of  
366 actual wadi flows across the aquifer. Little river water is lost as wadis flow over non-aquifer rocks,  
367 but losses through wadi floors occur across the Quaternary aquifer. The rate of modelled wadi  
368 recharge depends on the volume and duration of wadi flows, and is highest along the southwest and  
369 western edges of the main irrigated area (Figure 12). There is little wadi recharge north of Chahaertan,  
370 where the river channel usually flows only once or twice a year, and at a lower rate. Modelled  
371 recharge volumes are shown in Table II and indicate that wadi losses and irrigation returns provide  
372 the majority of recharge to the entire Quaternary aquifer, and dominate recharge in the vicinity of  
373 Chahaertan.

374

375 The steady state groundwater flow model, with input from the recharge model and available aquifer  
376 parameters, represents the groundwater head distribution across the aquifer relatively closely (Figure  
377 13). This improves confidence in our understanding of the Chahaertan groundwater system,  
378 supporting the limited available hydrogeological data and implying that the recharge and flow  
379 processes inferred from hydrodynamic and hydrogeochemical (including residence time) analysis are  
380 plausible. Although the lack of data, and in particular daily rainfall, means that fully a refined  
381 historical simulation is not yet possible, a dynamic balance model reproduces the general pattern of  
382 observed annual groundwater level variations and the observed groundwater level fall over the period  
383 of irrigation development, further improving confidence in our understanding of the groundwater

384 system (Ó Dochartaigh and MacDonald 2006). If the decline continues at the same rate, production  
385 wells may start to show falling yields within 20 to 30 years, and the shallowest wells (100 m deep)  
386 may need to be abandoned within 40 years.

387

## 388 **Discussion**

389

390 The combined study of hydrodynamics, hydrochemistry (including residence times) and subsequent  
391 testing with a groundwater recharge and flow model has helped unravel the processes of groundwater  
392 degradation in the Chahaertan irrigated area. Of particular importance is the change in recharge  
393 processes during the development of the area.

394

### 395 *Predevelopment*

396 Before irrigation development at Chahaertan, surface and groundwater flowed largely uninterrupted  
397 from the Helan Mountains to the Jilantai lake. The presence of CFC, isotopic signature, and lack of  
398 increased salinity in pre-development groundwater at Chahaertan indicate that active local wadi  
399 recharge occurred within the last 50 years, and before the onset of irrigation returns in the late 1970s.  
400 Model results confirm that infiltration occurred along the wadi channels between the Helan Mountains  
401 and Chahaertan, but was significantly enhanced at Chahaertan. This was caused by annual overbank  
402 flooding, which helped develop the soils that support agriculture Chahaertan. This study is the first to  
403 emphasise the importance of local recharge at Chahaertan. Previous theories held that most recharge  
404 to the aquifer basin occurred at the edge of the Helen Mountains, with subsequent slow subsurface  
405 flow to Chahaertan over thousands of years. The new modelling and geochemical studies show that,  
406 although this mechanism may be occurring, it is not the dominant influence on the groundwater  
407 system.

408

409 Groundwater modelling indicates that from Chahaertan northwards, subsurface flow dominates water  
410 movement to Jilantai. This is corroborated by residence time data, as groundwater further down the

411 flow line does not show detectable CFCs, and there is no evidence of active recharge for at least the  
412 past 50 years. The depletion in  $\delta^2\text{H}$  and  $\delta^{18}\text{O}$  in groundwaters is likely to be the product of mixing  
413 between a late-Pleistocene end-member, with a depleted isotopic composition indicating cooler  
414 recharge conditions, and younger Holocene water (up to 10 kyr) old that has an essentially modern  
415 isotopic composition. This is similar to results from other parts of northern China (e.g. Chen et al  
416 2003, Ma and Edmunds 2006), and is consistent with modelled groundwater travel times thousands of  
417 years through the aquifer to Jilantai. The one exception is at Jilantai lake itself, where mixing with re-  
418 infiltrating lake water appears to have led to the presence of CFCs in groundwater.

419

420 Pre-development groundwater chemistry at Chahaertan is likely to have been similar to that of  
421 groundwater today in the surrounding non-irrigated area: moderately mineralised (TDS ~400 mg/L),  
422 Ca-Mg dominated waters with slightly alkaline pH, and less than 5 mg/L  $\text{NO}_3\text{-N}$ . This is comparable  
423 to studies elsewhere in semi-arid northwest China, where groundwaters unaffected by agriculture or  
424 industry have an average TDS of <300 mg/l and  $\text{NO}_3\text{-N}$  concentration of 7.3 mg/l (Guo and Wang  
425 2004). Further down the groundwater flow line towards Jilantai, groundwater has evolved to become  
426 more alkaline and reducing, with cation exchange and halite dissolution being the prominent  
427 processes.

428

429 *Present day*

430 The present day groundwater system in Chahaertan has evolved significantly since irrigation started,  
431 and annual abstraction is now in the range 19–21 Mcm (Figure 14). There have been two major  
432 effects on the groundwater system: declining water levels and a marked decrease in water quality.  
433 This degradation has been exacerbated by engineering works to prevent virtually all seasonal over-  
434 bank flooding, which has greatly reduced wadi recharge. Groundwater levels have fallen by up to  
435 0.5 m/yr for at least 20 years. Examining this decline in greater spatial detail with a dynamic balance  
436 groundwater flow model, using a factored sequence of the available groundwater abstraction,  
437 confirms that water level decline in the main Chahaertan irrigated area has decreased slightly since the  
438 1990s. This has corresponded with the change of focus for groundwater development to Little



439 Chahaertan. However, if the decline continues at the same rate, production wells may start to show  
440 declining yields within 20 to 30 years, and the shallowest wells (100 m deep) are likely to have to be  
441 abandoned within 40 years.

442

443 The direct relationship between CFC concentrations and the degree of groundwater mineralisation  
444 (represented by TDS, Figure 11) clearly demonstrates that recycling of irrigation water is causing  
445 groundwater degradation, with a marked increase in salinity (a TDS increase from 400 mg/L up to  
446 700-1900 mg/L) and an increase in nitrate concentrations (as N) from <5 mg/L up to 137 mg/L. The  
447 fact that re-infiltration of irrigation water has almost overtaken river infiltration as the main source of  
448 recharge in some areas has radically changed the chemistry of the local groundwater system. The  
449 majority of the wells within the irrigated area show elevated nitrate and salinity, as well as enrichment  
450 in Ca, Cl, SO<sub>4</sub> and Mg (Table ESM2, Figure 5). The generally slow movement of groundwater  
451 through the aquifer, which is supported by the modelling results, means there is a long lag time  
452 between cause and effect. It is likely that poor quality water from irrigation returns, which is moving  
453 downwards through the thick unsaturated zone (between 45 and 75 m thick in 2006), will continue to  
454 degrade groundwater quality in the aquifer for tens of years as it reaches the water table.

455

## 456 **Conclusions**

457

458 A combination of hydrodynamic and hydrogeochemical (including residence time) analysis and  
459 numerical groundwater modelling has provided a detailed insight into groundwater degradation in an  
460 irrigated area in semi-arid northern China, and by inference in other similar irrigated areas. An  
461 improved conceptual model of the groundwater system has revealed its complex nature and the  
462 multifold impacts of human activity.

463

464 Previous theories held that the main groundwater input at Chahaertan was subsurface flow from the  
465 southeastern boundary of the aquifer basin, recharged from runoff from the Helan Mountains. New

466 evidence from this study shows that the main groundwater input in pre-development times was  
467 focussed river recharge in and around the now-irrigated area. Flood-prevention engineering works  
468 since development began have significantly reduced this recharge. Returns from inefficient flood  
469 irrigation have partially compensated (by volume) for the reduction in natural recharge, but  
470 abstraction nonetheless exceeds recharge, and groundwater levels continue to fall by up to 0.5 m/yr.  
471 Irrigation returns now comprise the largest proportion of local recharge.

472

473 The close relationship between the degree of groundwater mineralisation and the proportion of  
474 modern water, shown by CFC concentrations, clearly demonstrates that recycling of irrigation water is  
475 causing groundwater degradation.

476

477

#### 478 **Acknowledgements**

479 This study was funded by the Australian Agency for International Development (AusAID), A\$10  
480 million, 2001-06, Alxa League Environmental Rehabilitation and Management Project (ALERMP).

481 This paper is published with the permission of the Director, ALERMP and the Executive Director of  
482 the British Geological Survey (NERC).

483

484 **References**

- 485 Allen RG, Pereira LS, Raes D and Smith M., 1998. Crop evapotranspiration: guidelines for computing crop  
486 water requirements. FAO Irrigation and Drainage Paper no. 56, Rome, Italy.
- 487 Busenberg E and Plummer L. 1992. Use of Chlorofluorocarbons (CCl<sub>3</sub>F and CCl<sub>2</sub>F<sub>2</sub>) as Hydrologic Tracers and  
488 Age-Dating Tools: The Alluvium and Terrace System of Central Oklahoma, Water Resources Research  
489 28(9), 2257-2283.
- 490 Chen Z, Qi J, Xu J, Xu J, Ye H and Nan Y. 2003. Paleoclimatic interpretation of the past 30 ka from isotopic  
491 studies of the deep confined aquifer of the North China plain. Applied Geochemistry 18, 997-1009
- 492 Chen J, Tang C, Sakura Y, Yu J and Fukushima Y. 2005. Nitrate pollution from agriculture in different  
493 hydrogeological zones of the regional groundwater flow system in the North China Plain.  
494 Hydrogeology Journal 13: 481-492
- 495 Edmunds W M, Ma J, Aeschbach-Hertig W & Darbyshire D P F. 2006. Groundwater recharge history and  
496 hydrogeochemical evolution in the Minqin Basin, North West China. Applied Geochemistry 21, 2148-  
497 2170.
- 498 Foster S, Garduno H, Evans R, Olson D, Tian Y, Zhang W and Han Z. 2004. Quaternary Aquifer of the North  
499 China Plain – assessing and achieving groundwater resource sustainability. Hydrogeology Journal 12:  
500 81-93.
- 501 Gates J B, Böhlke J K and Edmunds W M. 2008. Ecohydrological factors affecting nitrate concentrations in a  
502 phreatic desert aquifer in northwestern China. Environmental Science & Technology 42: 3531–3537.
- 503 Groundwater Development and Utilisation Teaching and Research Office. 1984. Hydrogeology Survey Report  
504 on Chahaertan Irrigation Area, Left Banner: Water Resource Assessment and Systematic Analysis.  
505 Produced within the Agricultural and Animal Husbandry, Water Conservancy and Engineering School  
506 of the Inner Mongolia Agricultural and Animal Husbandry College. December 1984.
- 507 Guo H and Wang Y. 2004. Hydrogeochemical processes in shallow quaternary aquifers from the northern part  
508 of the Datong Basin, China. Applied Geochemistry 19: 19-27.

- 509 Hughes A G, Mansour M M, Robins N S and Peach D W. 2006. Numerical modeling of runoff recharge in a  
510 catchment in the West Bank. In: *MODFLOW and More: Managing Ground-Water Systems –*  
511 *Conference Proceedings*. Colorado School of Mines, May 2006, Volume 1: 385-389.
- 512 Hughes A G, Mansour M M and Robins N S. 2008. Evaluation of distributed recharge in an upland semi-arid  
513 karst system: the West Bank Mountain Aquifer. *Hydrogeology Journal*, 16: 845-854.
- 514 Jerie P. 2006. Improving the Management of Water and Nitrogen Fertilizer for Agricultural Profitability and  
515 Groundwater Quality in Alxa. Preliminary ALERMP Report, June 2006.
- 516 Jackson C R, Hughes A G, Ó Dochartaigh B É, Robins N S and Peach D W. 2005. Numerical testing of  
517 conceptual models of groundwater flow: A case study using the Dumfries Basin Aquifer. *Scottish*  
518 *Journal of Geology*, vol. 41 (1), 51-60.
- 519 Ji X B, Kang E S, Chen R S, Zhao W Z, Zhang Z H and Jin B W. 2006. The impact of the development of water  
520 resources on environment in arid inland river basins of Hexi region, Northwestern China.  
521 *Environmental Geology* 50 (6): 793-801.
- 522 Kendy E, Gerard-Marchant P, Walter M T, Zhang Y, Liu C and Steenhuis T S. 2003. A soil-water-balance  
523 approach to quantify groundwater recharge from irrigated cropland in the North China Plain.  
524 *Hydrological Processes* 17, 2011-2031.
- 525 Kreuzer A M, Von Rohden C, Friedrich R, Chen Z, Shi J, Hajdas I, Kipfer R, and Aeschbach-Hertig W. 2009. A  
526 record of temperature and monsoon intensity over the past 40 kyr from groundwater in the North China  
527 Plain. *Chemical Geology* 259, 168–180.
- 528 Lange J, Greenbaum N, Husary S, Ghanem M, Leibundgut C and Schick A P. 2003. Runoff generation from  
529 successive simulated rainfalls on a rocky, semi-arid, Mediterranean hillslope. *Hydrological Processes*  
530 17, 279-296
- 531 Left Banner Water Management and Water Resource Office. 1992. Water Supply Project (Supply Amount)  
532 Yield Statistics Summary Table. Alxa, Left Banner, Inner Mongolia,. December 1992.

533 Ma J Z, Wang X Z and Edmunds W M. 2005. The characteristics of ground-water resources and their changes  
534 under the impacts of human activity in the arid Northwest China - a case study of the Shiyang River  
535 Basin. JOURNAL OF ARID ENVIRONMENTS 61 (2): 277-295

536 Ma J Z and Edmunds W M. 2006. Groundwater and lake evolution in the Badain Jaran Desert ecosystem, Inner  
537 Mongolia. Hydrogeology Journal 14, 1231-1243.

538 Ó Dochartaigh B É and MacDonald A M. 2006. Groundwater degradation in the Chahaertan Oasis, Alxa  
539 League, Inner Mongolia. British Geological Survey Commissioned Report CR/06/220N.

540 People's Liberation Army. 1976. Regional Hydrogeological Survey Report for Sheet J-48-[4]: Jilantai.

541 People's Liberation Army. 1980. Regional Hydrogeological Survey Report for Sheet J-48-[10]: Alxa, Left  
542 Banner.

543 Rushton K R and Wedderburn L A. 1971. Starting Conditions for Aquifer Simulations. Ground Water 11 (1),  
544 37-42.

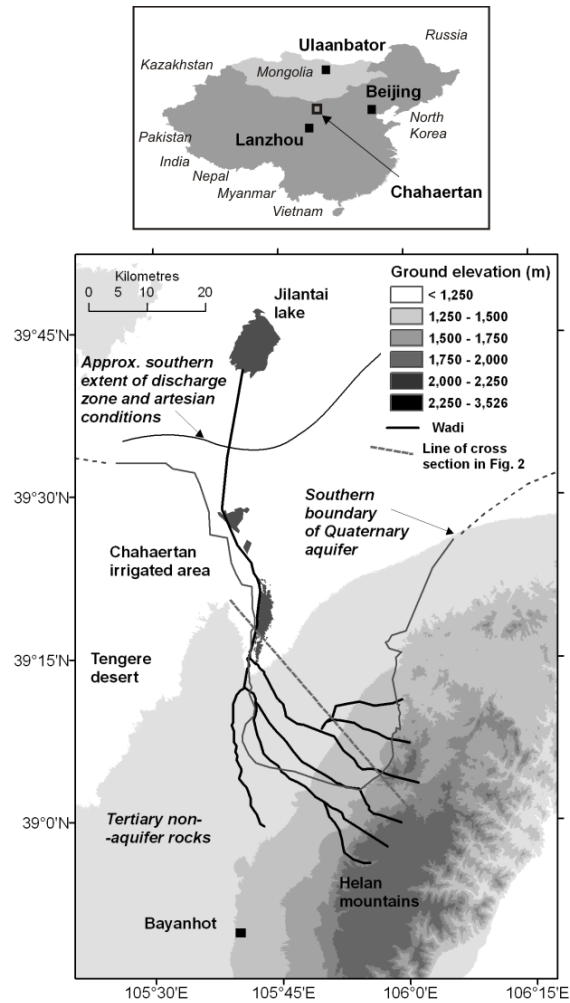
545 Spink A E F, Jackson C R, Hughes A G and Hulme P J. 2003. The Benefits of Object-Oriented Modeling  
546 Demonstrated through the Development of a Regional Groundwater Model. MODFLOW and More  
547 2003: Understanding through Modeling – Conference Proceedings, Poeter, Zheng, Hill and Doherty.  
548 pp 336-340.

549 Spink, A E F, Hughes A G, Jackson C R and Mansour M M. 2006. Object-oriented Design in Groundwater  
550 Modelling. MODFLOW and More 2006: Managing Ground-Water Systems – Conference  
551 Proceedings, Poeter, Hill and Zheng. Colorado School of Mines, USA.

552 Williams A. 2006a. Recommendations for improvements to livestock enterprises based on stall feeding in an  
553 oasis environment, with particular reference to Chahaertan. AusAID: ALERMP Project Report.

554 Yuan L J and Wu S Z. 1996. Groundwater Hydrological Systems in Arid Areas: Western Helanshan  
555 Groundwater Systems Research. Geological Press, Beijing.

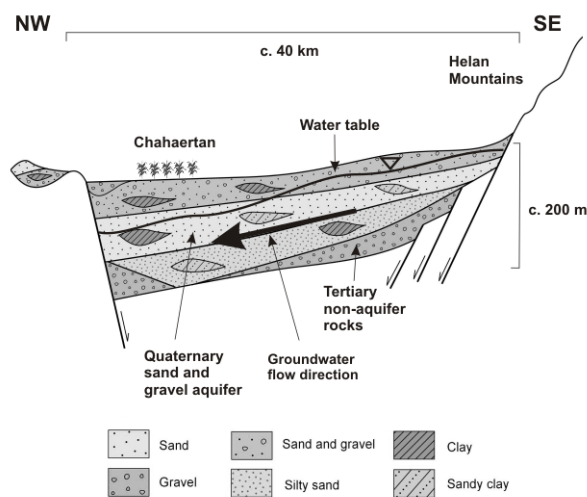
556



557

558 Figure 1 Location and generalised hydrology and hydrogeology of Chahaertan and the Quaternary aquifer.

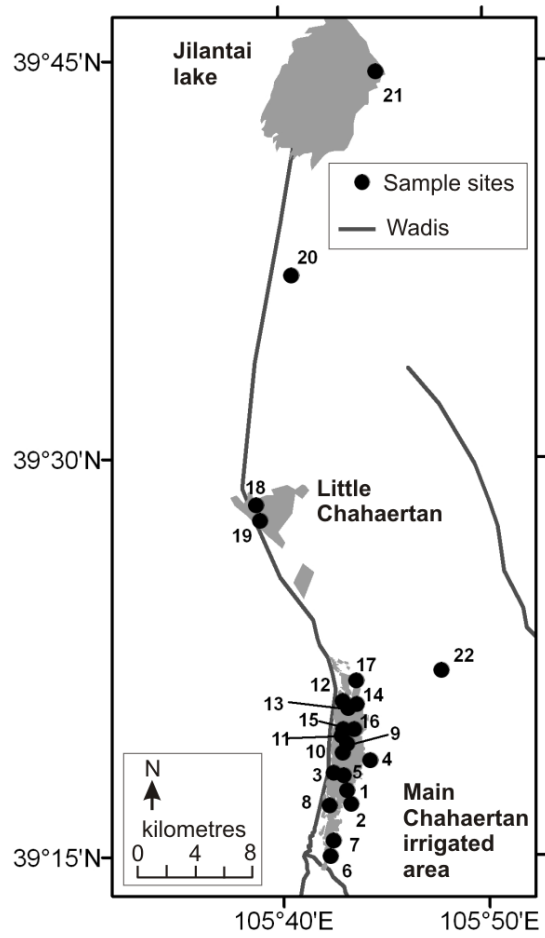
559



560

561 Figure 2 Schematic cross section of the Chahaertan Quaternary aquifer system along the line shown in

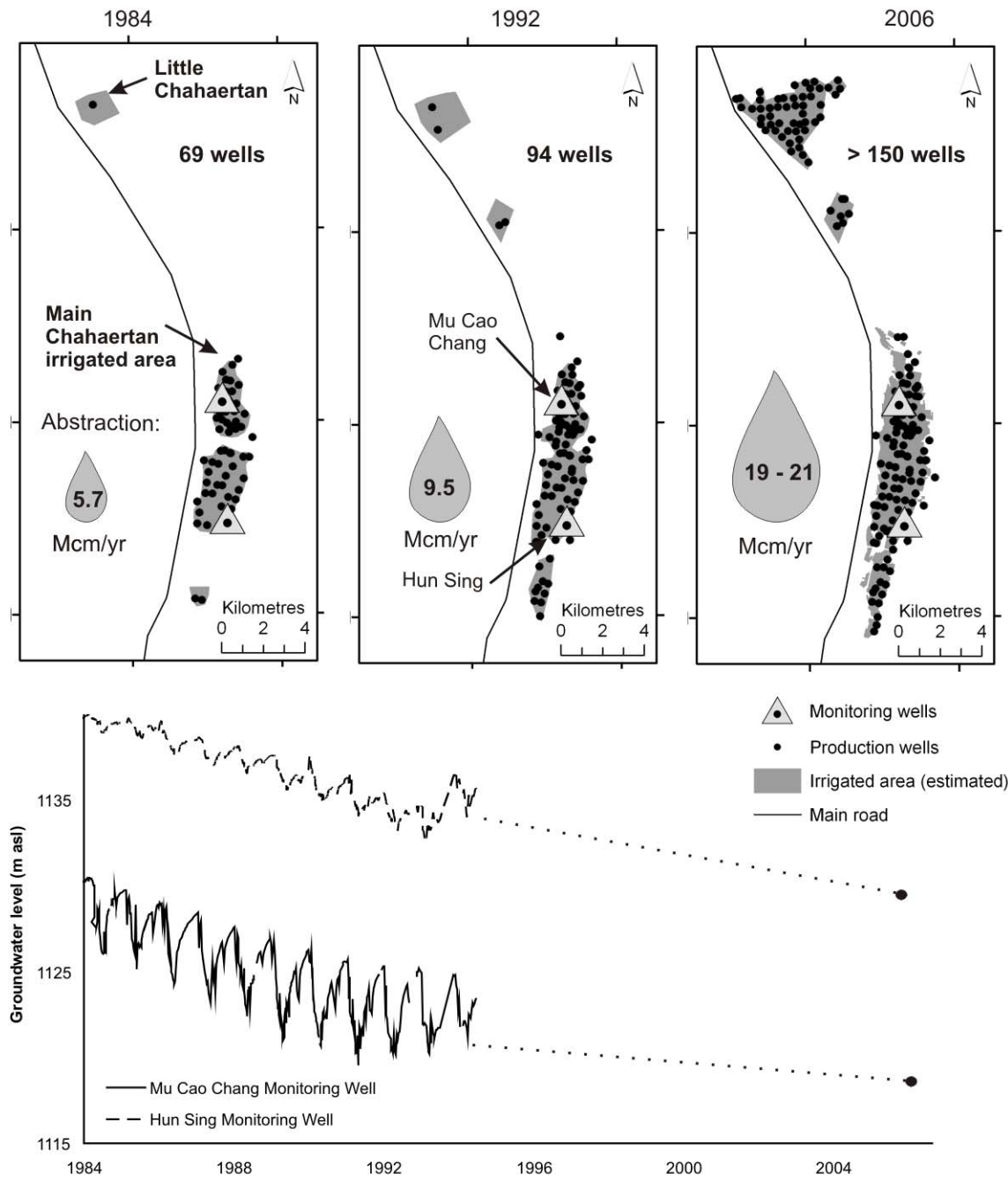
562 Figure 1, and showing the approximate position of the groundwater table



563

564 Figure 3 Location of groundwater chemistry sample sites at Chahaertan and the surrounding aquifer.

565 Sample numbers are as in Tables ESM1 – ESM3



566

567

Figure 4 Schematic illustrating the increase in irrigated area, number of production wells and

568

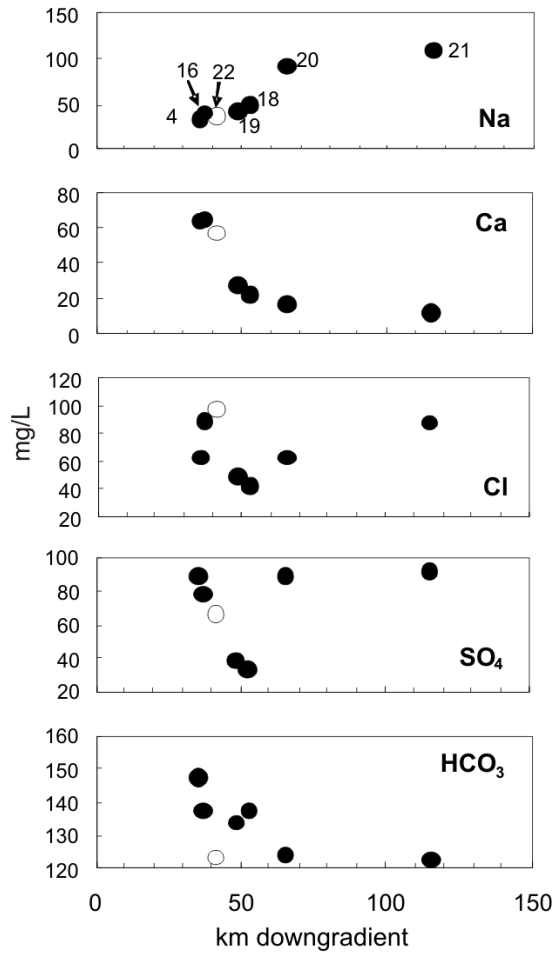
groundwater abstraction, and the simultaneous decline in groundwater levels at Chahaertan

569

from 1984 to 2006.

570





571

572

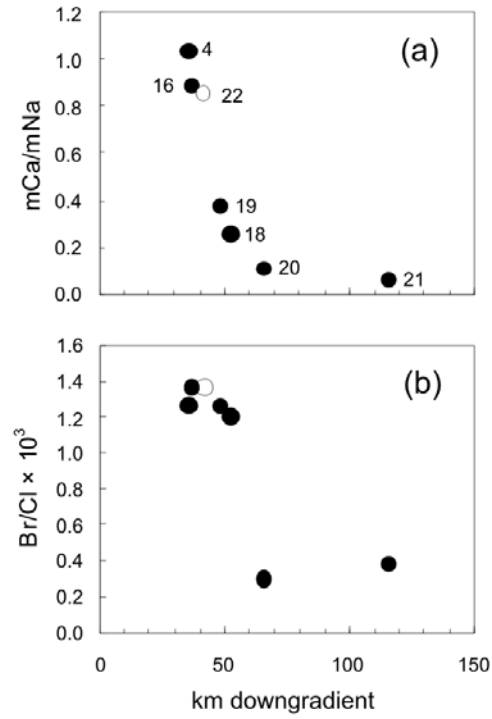
Figure 5

Major ion concentrations of pre-development Chahaertan groundwaters and groundwaters outside the irrigated area, plotted versus distance downgradient from the recharge area in the Helan Mountains. Site 22 lies off the assumed flowpath and is shown as an open circle. Sample location numbers are shown on the top (Na) plot.

573

574

575



576

577 Figure 6

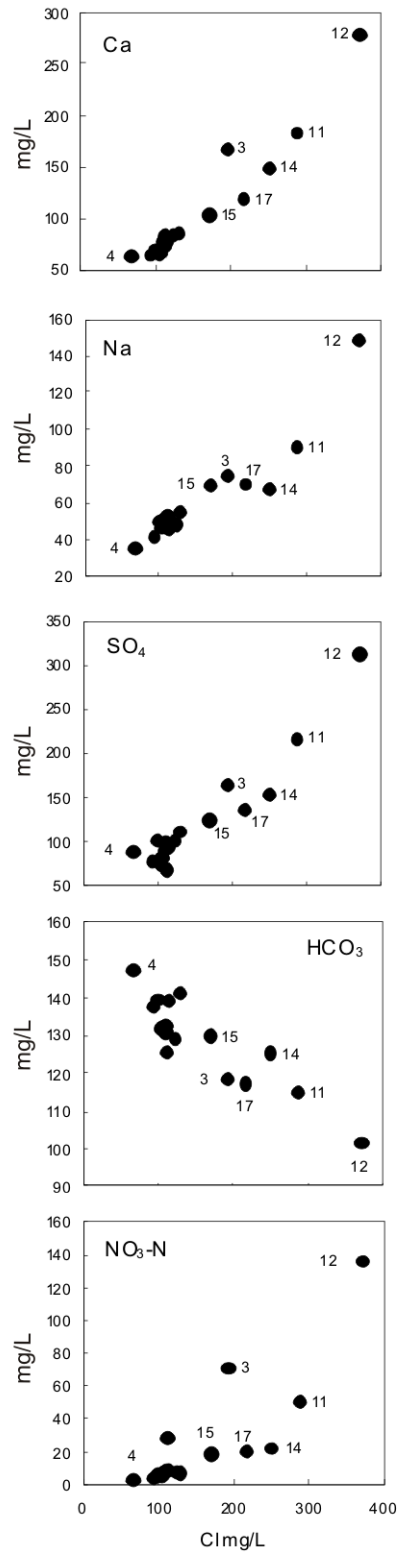
Plots of (a) Ca/Na molar ratios, and (b) Br/Cl ratios of baseline Chahaertan groundwaters and groundwaters outside the irrigated area, versus distance downgradient from the recharge area.

578

579

Site 22 lies off the assumed flowpath and is shown as an open circle.

580



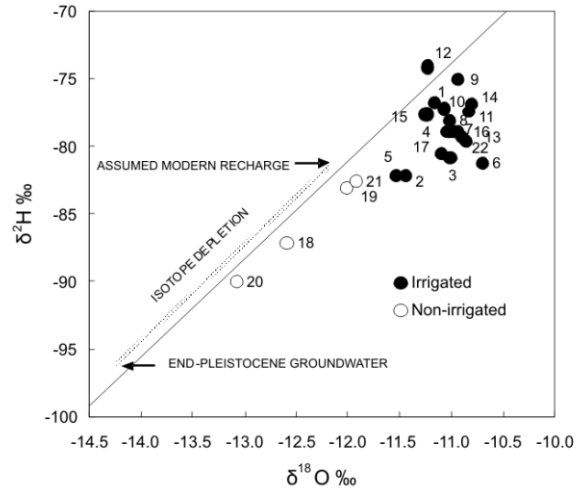
581

582

Figure 7

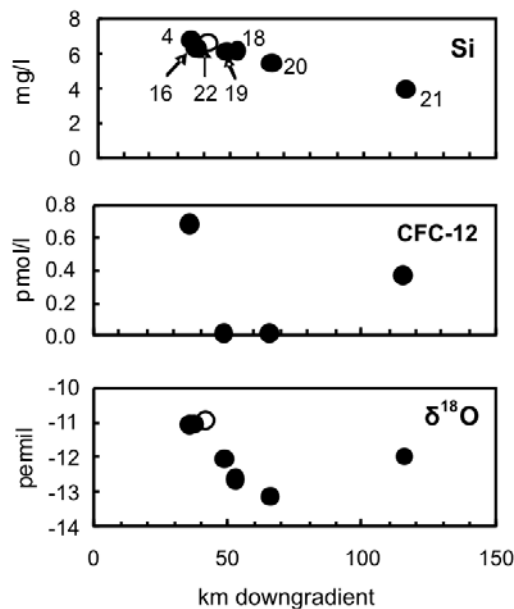
Plots versus Cl for the Ca, Na, SO<sub>4</sub>, HCO<sub>3</sub> and NO<sub>3</sub>-N contents of groundwaters from the irrigated area at Chahaertan. Selected site numbers shown.

583



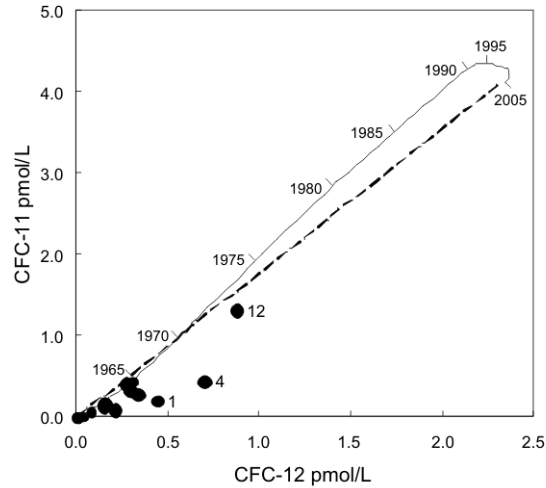
584  
 585  
 586  
 587  
 588  
 589  
 590  
 591

Figure 8 Plot of  $\delta^2\text{H}$  versus  $\delta^{18}\text{O}$  for all Chahaertan groundwaters within and outwith the irrigated area, with site numbers. The meteoric line (solid line) is for the nearest GNIP station at Yinchuan (longitude 106.13°E, latitude 38.29°N) (<http://nds121.iaea.org/wiser/index.php>) Yinchuan average isotope values are approximately  $-6.5$  ‰  $\delta^{18}\text{O}$  and  $-45$  ‰  $\delta^2\text{H}$ . The isotopic composition of end-Pleistocene groundwater is based on a 2‰ depletion in  $\delta^{18}\text{O}$ , as found by Kreuzer et al. (2009) in the North China Plain.



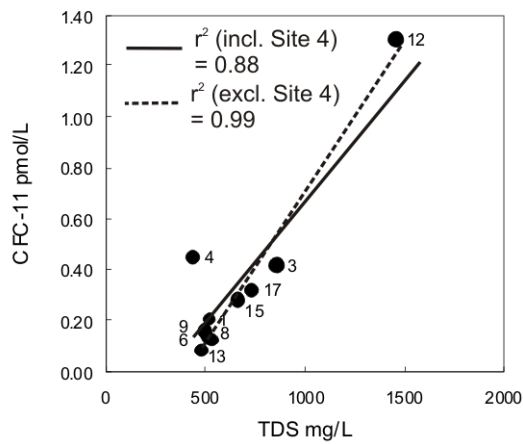
592  
 593  
 594  
 595

Figure 9 Plots of the Si, CFC-12 and  $\delta^{18}\text{O}$  values for pre-development Chahaertan groundwaters and groundwaters outside the irrigated area, plotted versus distance downgradient from the recharge area. Site 22 lies off the assumed flowpath and is shown by an open circle.



596

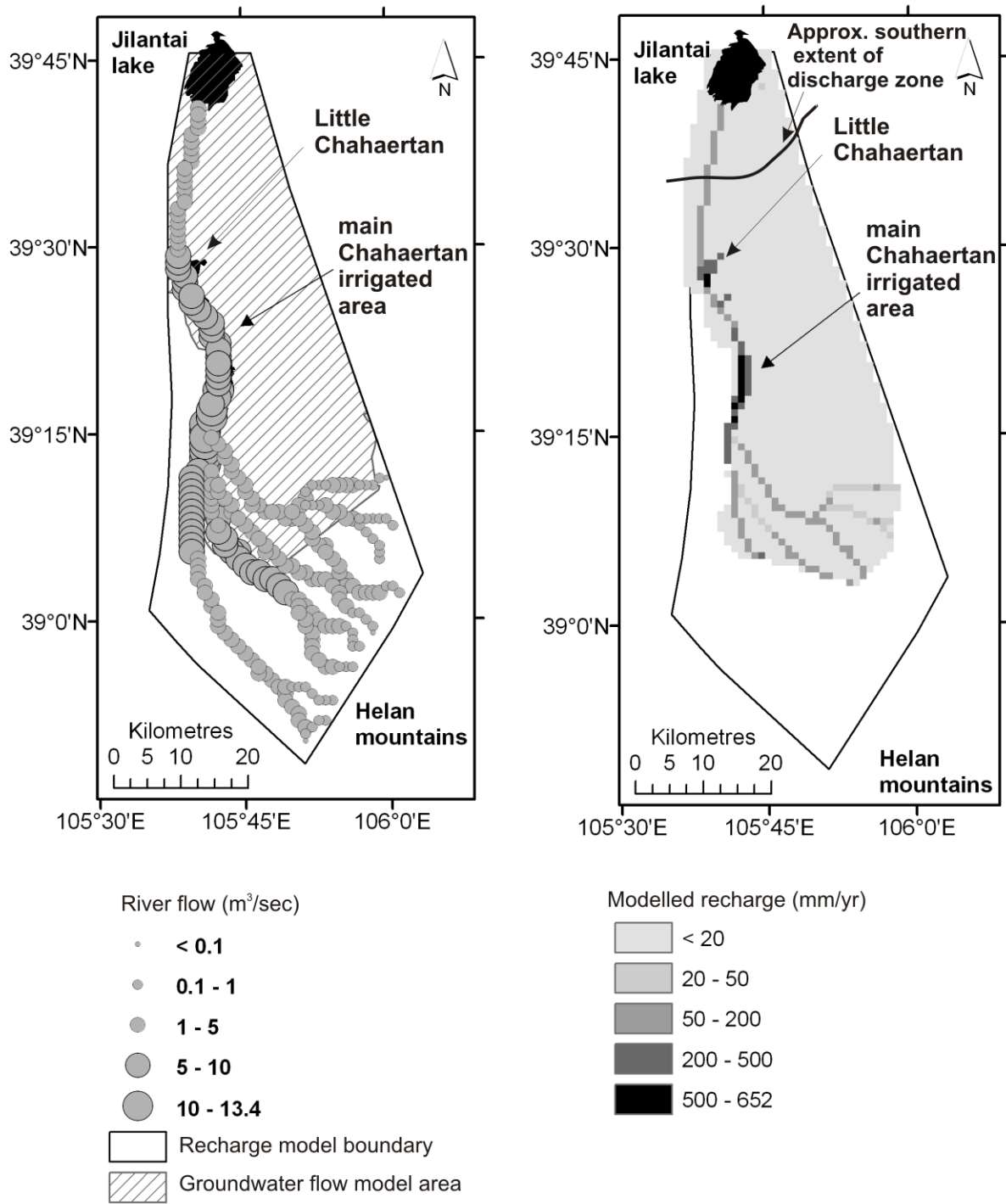
597 Figure 10 Plot of CFC-11 versus CFC-12 concentrations for Chahaertan groundwaters, with selected site  
 598 numbers. The piston flow (solid) curve is based on secular changes in the Northern Hemisphere atmospheric  
 599 mixing ratios over the past 50 years (data from [http://water.usgs.gov/lab/software/air\\_curve/](http://water.usgs.gov/lab/software/air_curve/)) and an average  
 600 unsaturated zone recharge temperature of 15°C at an elevation of 1100 m ASL. The dashed mixing line is  
 601 between modern and older CFC-free water.



602

603 Figure 11 Plot of CFC-11 versus TDS (total dissolved solids) for Chahaertan groundwaters. Selected  
 604 site numbers are shown.

605

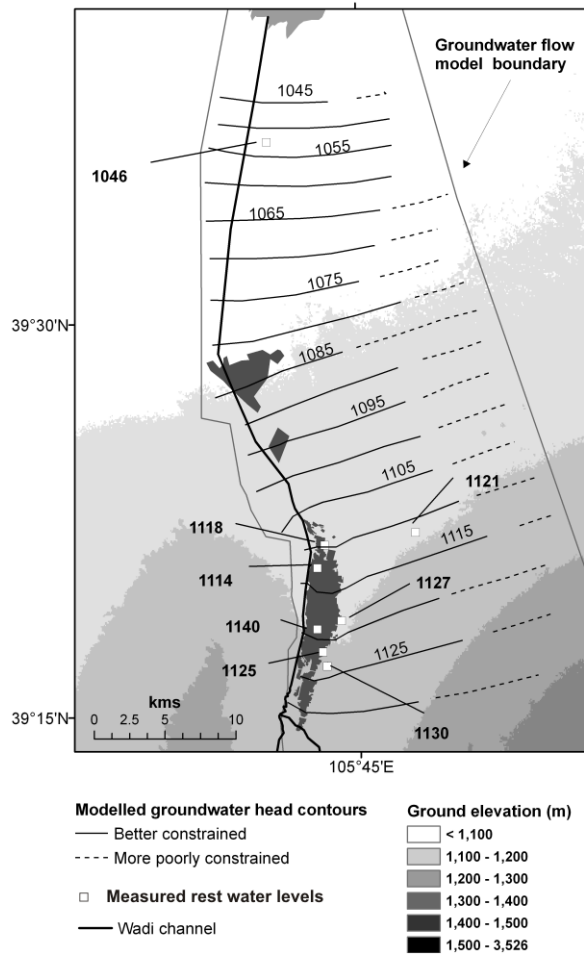


606

607 Figure 12 Simulated river flows for a large rainfall event (41 mm/day in the Helan Mountains) (left); and

608 spatial distribution of modelled recharge across the Chahaertan aquifer (right)

609

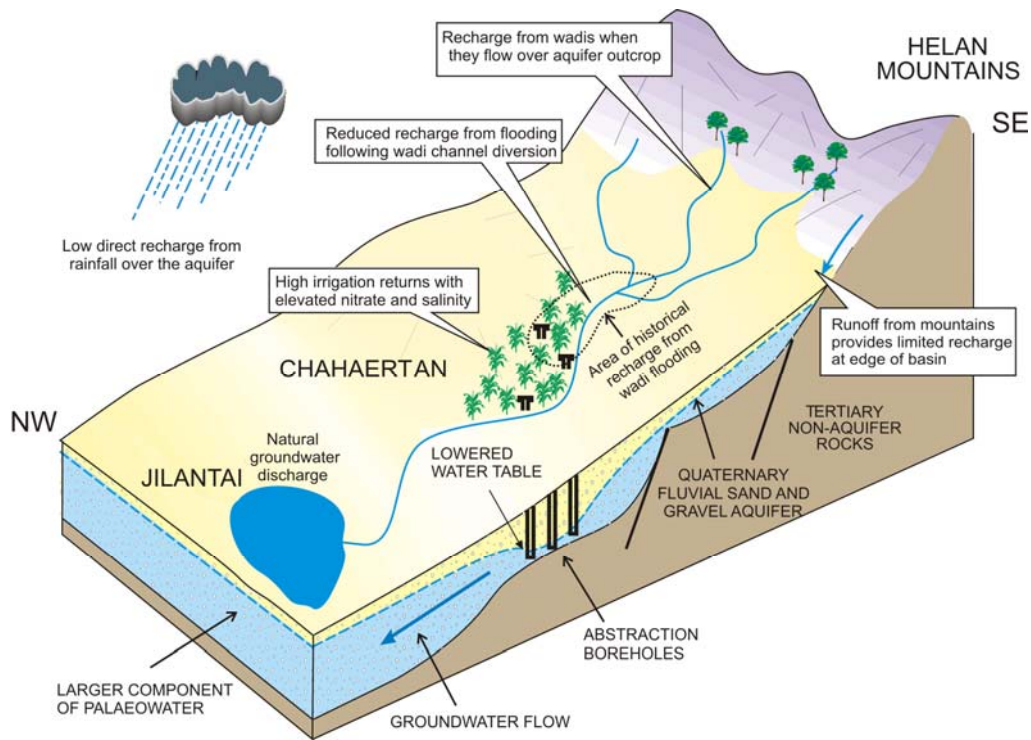


610

611 Figure 13

Modelled steady state groundwater head contours and available observed rest water levels in the aquifer around Chahaertan. All water levels in metres above sea level.

612



613

614 Figure 14 Conceptual model of post-development groundwater system at Chahaertan.

615

616

617 Table I Wadi channel characteristics

Wadi location	Channel width	Channel bed material	Annual flow events	Flow depth in channel	Roughness coefficient <sup>1</sup>
Helan Mountains	5 m	Coarse, high-energy gravel to boulder size deposits.	Unrecorded but likely to be 5-10 times, for >10 hours per event.	Average 0.5 m	0.05
Quaternary aquifer at Chahaertan	20-30 m	Fine sands and gravels.	3-4 times, for 3-10 hours per event. In smaller events, flow dies out c. 20 km north of Chahaertan.	Maximum 1 m, average 0.5 m	0.03
Quaternary aquifer at the lake at Jilantai	20-30 m	Fine sands.	2 times (maximum), for <5 hours per event.	Average 0.5 m	0.02

618 <sup>1</sup>Based on literature values for roughness coefficients for natural channels

619

620 Table II. Modelled recharge volumes at Chahaertan and across the Quaternary aquifer

Recharge source	Volume in Chahaertan local area (Mcm/a)	Volume across Quaternary aquifer (Mcm/a)
Rainfall	2	20
Wadi leakage	6	14
Irrigation returns	10	10
<b>Total</b>	<b>18</b>	<b>44</b>

621